Remote Sensing of Environment 177 (2016) 1–12

Contents lists available at ScienceDirect

Remote Sensing of Environment

journal homepage: www.elsevier.com/locate/rse

Trends and variability in extended ocean color time series in the main reproductive area of the Argentine hake, *Merluccius hubbsi* (Southwestern Atlantic Ocean)

Marina Marrari [a,b,c,*], Alberto R. Piola [a,b,c,d], Daniel Valla [a,b,c,d], John G. Wilding [e]

[a] Departamento de Oceanografía, Servicio de Hidrografía Naval, Av. Montes de Oca 2124, C1270ABV Ciudad Autónoma de Buenos Aires, Argentina
[b] Consejo Nacional de Investigaciones Científicas y Técnicas, Godoy Cruz 2290, C1425FQB, Ciudad Autónoma de Buenos Aires, Argentina
[c] Instituto Franco-Argentino sobre Estudios de Clima y sus Impactos, Universidad de Buenos Aires, Ciudad Autónoma de Buenos Aires, Argentina
[d] Departamento de Ciencias de Atmósfera y los Océanos, Facultad de Ciencias Exactas y Naturales, Universidad de Buenos Aires, Ciudad Autónoma de Buenos Aires, Argentina
[e] NASA Goddard Space Flight Center, 8800 Greenbelt Rd, Greenbelt, 20771, MD, USA

ARTICLE INFO

Article history:
Received 3 March 2015
Received in revised form 23 January 2016
Accepted 4 February 2016
Available online 18 February 2016

Keywords:
Ocean color
SeaWiFS
MODIS
Time series
Merluccius hubbsi

ABSTRACT

The Argentine hake *Merluccius hubbsi* is one of the main commercial resources of the Southwest Atlantic region, with a reported catch of 259,202 tons in 2014. Hake recruitment shows high interannual variability, yet the environmental and biological factors that influence reproduction are not fully understood. The increasing availability of ocean color data presents an opportunity to investigate a wide variety of fundamental topics including ocean primary productivity, climate change, and fisheries, among others. However, differences in the timing, length, and radiometer characteristics of the different missions result in a number of relatively short data records that are not suitable, individually, for the analysis of interdecadal changes. The combination of these datasets to produce longer time series of consistent data is essential for interpreting variability and trends in key parameters. We analyzed almost 5 years of high spatial resolution overlapping data from the SeaWiFS and MODIS Aqua sensors in the Southwestern Atlantic Ocean to assess differences in chlorophyll concentration retrievals, estimate uncertainties, and develop corrections. Data from SeaWiFS (1997–2006) and corrected MODIS (2007–2015) were analyzed jointly as a >17-year time series of consistent and continuous chlorophyll concentration data, the longest record to date in the region. Trend analyses performed in the main spawning and nursery areas of *M. hubbsi* revealed significant increases in chlorophyll concentrations since 1997. The environmental factors likely influencing the observed changes and the potential implications for recruitment of *M. hubbsi* are discussed.

1. Introduction

The Southwestern Atlantic Ocean (SWA) between 30 and 48°S is a dynamic area influenced by water masses of subantarctic origin modified by mixing from winds and tides. The Malvinas Current (MC) is a branch of the Antarctic Circumpolar Current and transports cold nutrient-rich waters northward along the shelf break of the Argentine Sea, while the Brazil Current (BC) transports warmer nutrient-poor waters southward (Peterson & Whitworth, 1989; Piola & Gordon, 1989). Both currents meet at approximately 38°S in the Brazil–Malvinas Confluence (BMC), generating one of the most dynamic areas of the world's ocean. Several frontal systems have been described in the continental shelf and shelf-break areas south of 30°S (Acha, Mianzán, Guerrero, Favero, & Bava, 2004; Saraceno, Provost, Piola, Bava, & Gagliardini, 2004; Romero, Piola, Charo, & Garcia, 2006; Rivas & Pisoni, 2010), many of which have been associated with spawning and feeding of higher trophic level organisms, including species of ecological and commercial importance such as squid, anchovy, and hake (Sánchez & Martos, 1989; Ehrlich & de Ciechomski, 1994; Brunetti, Ivanovich, Aubone, & Rossi, 2000, Bezzi et al., 2004; Marrari et al., 2013).

The Argentine hake *Merluccius hubbsi* occurs from southern Brazil to the south of Argentina (34–55°S) between 50 and 500 m depth. *M. hubbsi* is the dominant demersal fish of the region in terms of biomass and one of the main commercial resources, with a total catch of 259,202 tons reported in 2014 in the Argentine Sea, representing more than 50% of the total fish catch in the region (http://www.minagri.gob.ar). Two main stocks have been identified: a northern stock between 34° and 41°S, and a southern or Patagonian stock between 41° and 55°S, which accounts for 85% of the hake biomass in the Argentine Sea. Hake is a batch spawner with high reproductive activity from December to March and peaks in January–February (Macchi, Pájaro, & Ehrlich, 2004; Pájaro, Macchi, & Martos, 2005).

* Corresponding author at: Departamento de Oceanografía, Servicio de Hidrografía Naval, Av. Montes de Oca 2124, C1270ABV Ciudad Autónoma de Buenos Aires, Argentina.
E-mail address: mmarrari@hidro.gov.ar (M. Marrari).

http://dx.doi.org/10.1016/j.rse.2016.02.011

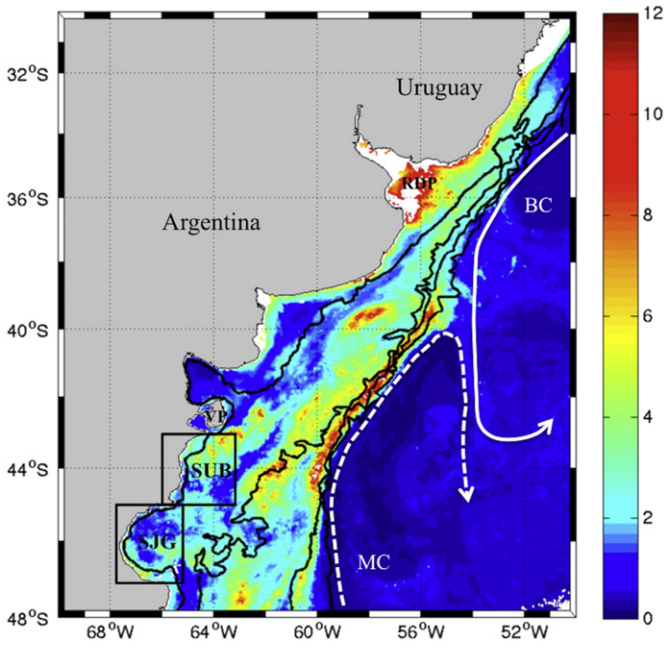

Fig. 1. Distribution of monthly mean surface chlorophyll concentration in the study area during November 2002 (SeaWiFS, mg m^{-3}, 2 km $pixel^{-1}$). The subareas SUB and SJG are indicated. MC = Malvinas Current, BC = Brazil Current, RDP = Rio de la Plata, VP = Valdés Peninsula. Black lines represent the 50, 100, 200 and 1000 m isobaths.

Large concentrations of eggs and larvae are often observed in the area south of Valdés Peninsula (SUB, Fig. 1), between 43 and 45°S in coastal and mid-shelf waters, whereas young juveniles are mostly present within the San Jorge Gulf (SJG), where food is abundant and circulation is more retentive than in mid-shelf areas (Palma, Matano, & Piola, 2008). The location of the spawning area is well documented and matches a bottom thermal front located parallel to the coastline at <80 m depth (Pájaro et al., 2005; Macchi, Martos, Reta, & Dato, 2010). This front is part of the highly productive Valdés Peninsula tidal front system (Acha et al., 2004), which is forced by the seasonal thermal stratification and high tidal energy dissipation characteristic of this area (Glorioso, 1987; Sabatini & Martos, 2002). The SJG covers a surface of 27,200 km^2 and is a semi-enclosed basin with a deep connection to the open shelf (Tonini, Palma, & Rivas, 2006). The area is characterized by vertical mixing by wind and tides, the input of southern coastal waters, and the presence of frontal systems.

There is great interannual variability in recruitment of *M. hubbsi* with important implications for fisheries in the region; however, the factors that control this variability are not fully understood. *M. hubbsi* reaches sexual maturity at 2–3 years old (Simonazzi, 2003) but the highest mortality occurs during the first year. For fish in general, the strength of a year class is mainly controlled by food availability during the larval period (Hjort, 1914; Cushing, 1974). Larvae experiencing favorable feeding conditions will grow faster and attain a larger size, reducing predation mortality during the larval stage. *M. hubbsi* larvae prey on smaller zooplankton, mainly copepods <2 mm in length, while young juveniles incorporate larger planktonic prey (Viñas & Santos, 2000; Temperoni & Viñas, 2013; Temperoni, Viñas, & Buratti, 2013). Variability in chlorophyll concentrations in the main reproductive area will likely have an influence on the reproductive success of hake via changes in the production of adequate prey.

Since the launch of the Sea-viewing Wide Field-of-view Sensor (SeaWiFS, McClain et al., 1998) onboard the Orbview-II satellite in August 1997, ocean color data products, in particular concentrations of chlorophyll *a* (CHL, mg m^{-3}) in the surface ocean, have been used to investigate a wide variety of fundamental topics including ocean primary productivity, biogeochemistry, coastal upwelling, eutrophication, and harmful algal blooms (*e.g.*, Muller-Karger et al., 2004; Hu et al., 2005). Other ocean color missions, such as the ongoing MODerate resolution Imaging Spectroradiometer (MODIS, Esaias et al., 1998) and the latest Visible Infrared Imager Radiometer Suite (VIIRS), provide continuity of remotely sensed ocean color products that is important for assessing the long-term global change in several key environmental parameters.

The proliferation of ocean color missions presents an opportunity for a number of oceanographic and ecological applications; nevertheless, differences in the timing and length of the different missions result in a number of relatively short data records that are not suitable, individually, for the analysis of interdecadal changes. There is a need for longer time series, which can be obtained by combining these shorter datasets; however, it has been long recognized that creating a consistent ocean color dataset from independent time series is challenging (McClain, 2009). In addition to differences in temporal coverage, variations in sensor design, calibration strategies, algorithm formulations, and band wavelength further amplify differences in the final satellite products that make it difficult to fully exploit the combined datasets.

The main objectives of this study are to 1) examine the agreement between SeaWiFS and MODIS Aqua CHL data in the Southwest Atlantic Ocean, 2) develop corrections to minimize differences between datasets and combine them to develop the longest possible time series of CHL in the area, and 3) analyze variability and trends in the main reproductive area of *M. hubbsi*. The results of these analyses will increase our understanding of the variability observed in the recruitment of hake and contribute to improved management capabilities.

2. Materials and methods

The study area includes continental shelf and oceanic waters between 30 and 48°S and 50–70°W in the SWA. Within this larger area, the subareas delimited by 43–45°S and 63–66°W (SUB) and by 45–47°S and 65.5–67.7°W (SJG) (Fig. 1) are of special interest because they represent the main spawning and nursery areas for the Patagonian population of *M. hubbsi*, respectively.

Daily SeaWiFS Local Area Coverage (LAC) data with 1 km $pixel^{-1}$ spatial resolution are available for the period August 1997–December 2006 in our study area, although lower spatial resolution imagery (9 km $pixel^{-1}$) is available until December 2010, when the sensor stopped collecting data. The MODIS Aqua dataset includes the period July 2002–present at 1 km $pixel^{-1}$. Together, the SeaWiFS LAC and MODIS Aqua datasets provide over 17 years of high spatial resolution surface chlorophyll concentration measurements and almost 5 years of temporally overlapping data. Monthly composites of surface chlorophyll concentration (CHL, mg m^{-3}) were generated from SeaWiFS (SWF) and MODIS Aqua (AQ) data. All available high-resolution (~1 km $pixel^{-1}$) level 2 data were processed with the standard flags and empirical algorithms (OC4v4 for SeaWiFS and OC3M for MODIS, O'Reilly et al., 2000), binned and mapped to a 2 km $pixel^{-1}$ spatial resolution. Reprocessing versions 2013.0 and 2013.1.1 were used for SWF and AQ respectively. The spatial resolution of 2 km $pixel^{-1}$ was selected to better represent the variability within the subregions analyzed, especially considering the differences that can occur between adjacent pixels in frontal areas. Using the standard 9 km $pixel^{-1}$ products would have reduced the number of pixels by a factor of ~20. To reduce errors caused by digitization and random noise without losing spatial resolution, a 3 × 3 box around each pixel was selected to compute the mean chlorophyll concentration (Hu, Carder, & Müller-Karger, 2001). Chlorophyll concentrations <0.02 and >20 mg m^{-3} were excluded from all analyses. All data were weighed equally and monthly composites were generated for the period September 1997–December 2006 for SWF, and July 2002–February 2015 for AQ. Data are distributed by the Ocean Biology Processing Group (OBPG) at NASA's Goddard Space Flight Center.

A preliminary comparison of monthly CHL from SWF and AQ data for the overlapping period (2002–2006) revealed significant differences in the retrievals from both sensors (example in Fig. 2). In general, both

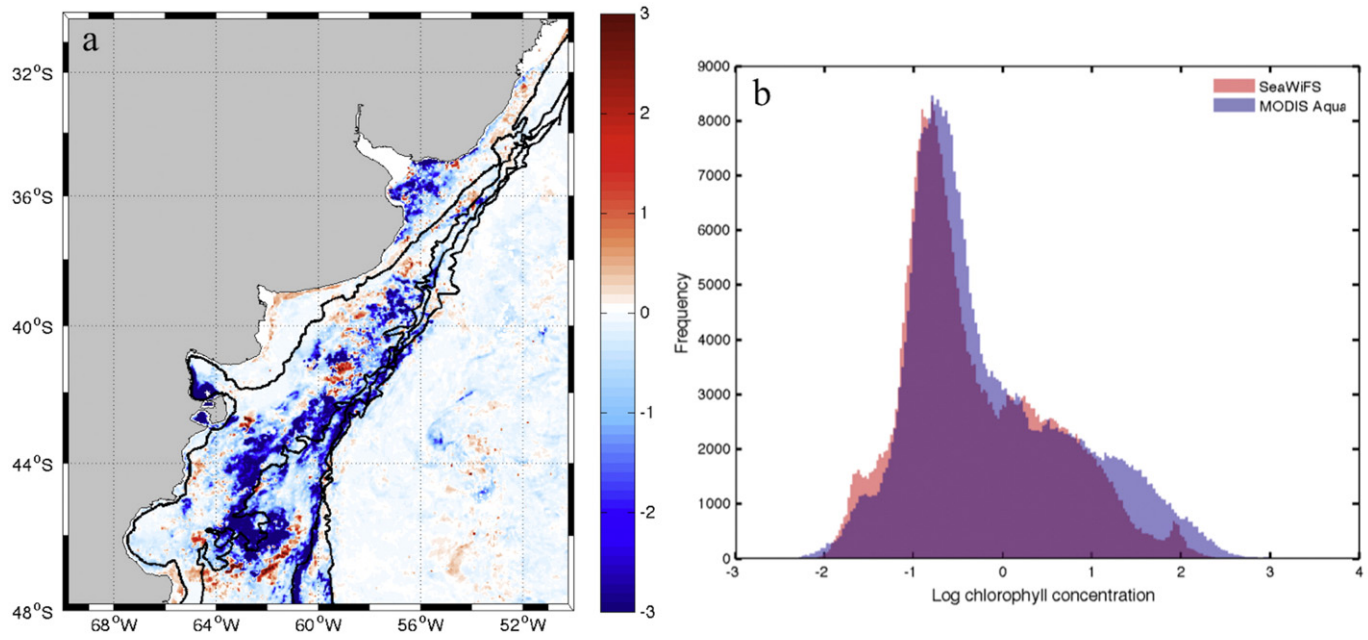

Fig. 2. a) Example of differences in monthly mean chlorophyll concentration retrievals between SeaWiFS and MODIS (SWF − AQ, mg m^{-3}) and b) frequency distribution of SWF (red) and AQ (blue) chlorophyll concentrations for all valid pixels in November 2004.

estimates agreed well at low chlorophyll concentrations (<1 mg m^{-3}) although in some instances SWF produced somewhat higher estimates than AQ, but AQ systematically produced larger estimates than SWF at higher chlorophyll concentrations. Based on the high productivity of our study area during spring and summer, and previous reports of SWF performing better than AQ at higher chlorophyll concentrations (*e.g.*, Werdell et al., 2009), the AQ dataset was corrected using SWF as reference. For this purpose, model II ordinary least squares (OLS) regressions (Legendre & Legendre, 1998) were calculated at each pixel on the log-transformed data using both monthly datasets for the period of overlap of both sensors (2002–2006, 54 months). Analyses with other types of fit indicated that applying higher order polynomials and other nonlinear fits did not reduce the errors. The relationship between retrievals from both sensors and their spatial variability were analyzed. Using the coefficients estimated from the regressions, corrections were applied at each pixel to the entire AQ time series (2002–2015). Because the natural distribution of chlorophyll concentrations is lognormal (Campbell, 1995), linear corrections and error estimates were made on the logarithmically transformed (base 10) data. Analysis of errors included root mean square error (RMS) and bias:

$$\text{log\_RMS} = \sqrt{\frac{\sum[\log(\text{AQ}) - \log(\text{SWF})]^2}{n}}$$

$$\text{log\_bias} = \frac{\sum[\log(\text{AQ}) - \log(\text{SWF})]}{n}$$

(Gregg & Casey, 2004; Marrari, Hu, & Daly, 2006). Errors were calculated for each pixel and mapped. In addition, errors were calculated for different CHL ranges for the subareas of interest SUB and SJG. Extended time series of monthly mean CHL were generated for both areas for the period 1997–2015 using SWF data for 1997–2006 and corrected AQ data for 2007–2015.

Trend analysis was performed jointly for the SWF and AQ datasets at all pixels following the methodology detailed in Saulquin et al. (2013). This method accounts for the noise autocorrelation in the time series, which affects the estimation of the uncertainty in the trend estimate and consequently the ability to detect a significant trend. The chlorophyll concentration time series, y_t, is modeled as a sum of three components: a long-term linear trend, a seasonal pattern, and a noise process:

$$y_t = \mu + \omega t + S_t + N_t, \quad t = 1....n$$

where n is the length of the time series, μ is the intercept term, ω is the linear trend, and S_t is the seasonal component (Weatherhead et al., 1998). N_t is the correlated noise, assumed to be first-order autoregressive process: $N_t = \phi N_{t-1} + \varepsilon_t$, where ε_t is a white noise and ϕ is the noise autocorrelation. Given a two-sensor dataset, we assume that both time series share the same long-term trend and seasonal pattern but involve an unknown level shift, δ, and correlated noise processes. The seasonal component is removed from all time series and the equations are then transformed to remove the autocorrelation (Cochrane & Orcutt, 1949). For periods when only one time series is present, the equations for SeaWiFS (y^*_{1t}) and MODIS (y^*_{2t}) are:

$$y^*_{1t} = \mu(1-\phi_1) + \omega\phi_1 + \omega(1-\phi_1)t + \varepsilon_{1t}$$
$$y^*_{2t} = \mu(1-\phi_2) + \omega\phi_2 + \omega(1-\phi_2)t + \delta(1-\phi_2) + \varepsilon_{2t}$$

where t is time relative to each time series. When both time series are present:

$$y^*_t = \mu(1-\alpha) + \omega(1-\alpha)t - \alpha\delta + \varepsilon_{3t}$$

with α representing the correlation between N_1 and N_2. The transformed equation can be expressed in matrix form as:

$$Y^* = X^* A + \varepsilon$$

where X^* is the $T \times 3$ coefficient matrix for the equation system, A is the parameter vector (μ, δ, ω), and ε is the residual white noise. The OLS estimator of A yields estimates of μ, δ, and ω. In practice the equation is solved with an iterative procedure until reaching convergence. The initial values for all parameters are evaluated from the data and A is estimated, then all parameters are revaluated. The variable $|\omega|/\sigma_\omega$ is used to detect significant trends, and the 95% confidence level is reached for $|\omega|/\sigma_\omega > 1.96$. Only trend estimates that satisfy the 95% detection threshold are considered. More details on the numerical resolution of the equations can be found in Tiao et al. (1990) and Saulquin et al. (2013).

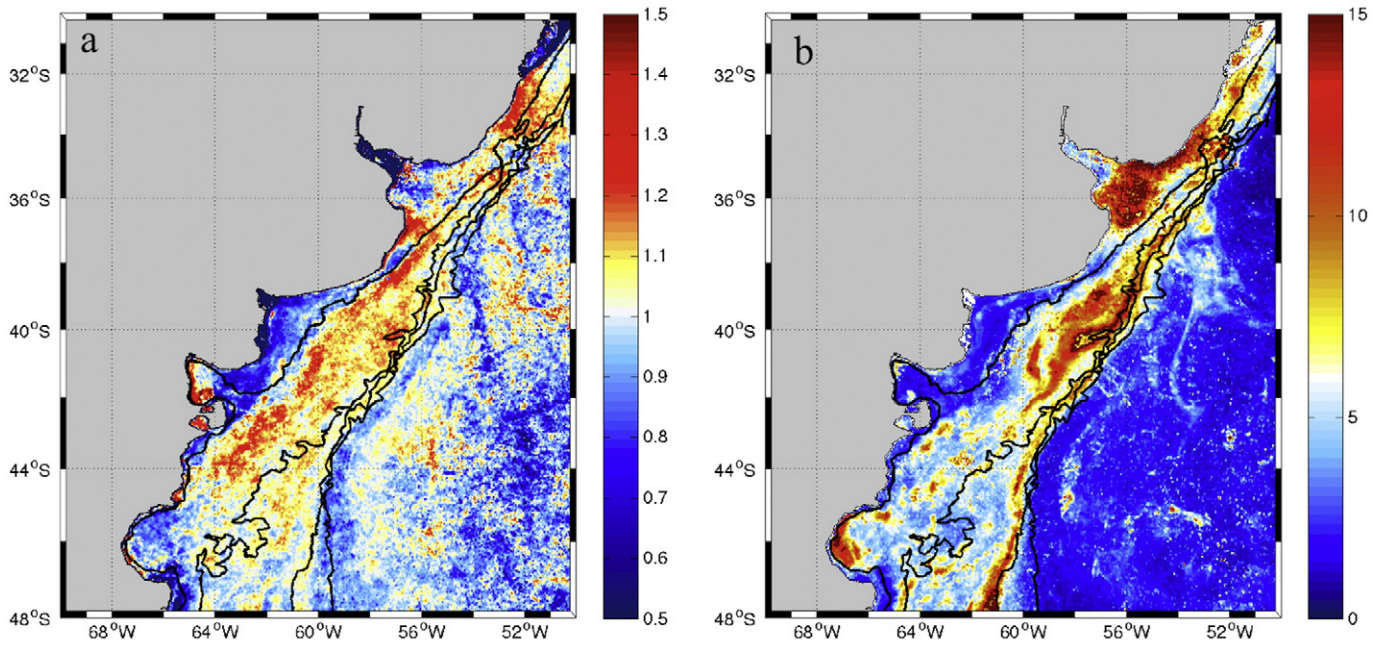

Fig. 3. Distribution of a) the slope of the regression log(SWF) *vs.* log(AQ) for 2002–2006 and b) annual CHL amplitude at each pixel from SWF monthly climatology data (maximum–minimum for 1997–2006). Black lines are the 50, 100, 200 and 1000 m isobaths.

3. Results

The relationship between sensor retrievals showed great spatial variability within the study area. The distribution of the slopes of the regressions at each pixel showed a well-defined pattern, with coastal areas <50 m depth and oceanic waters of the Malvinas Current characterized by slopes of the regression SWF *vs.* AQ generally close to or lower than unity, which indicates that in those areas SWF estimates were similar or larger than those produced by AQ (Fig. 3a). We note that the above regions present a relatively weak vertical stratification, even during the spring and summer seasons (*e.g.*, Bianchi et al., 2005; Romero et al., 2006). However, in seasonally stratified waters, such as the mid- and outer shelf, and oceanic areas characterized by elevated CHL such as the return of the Malvinas Current (Saraceno, Provost, & Piola, 2005), the slopes were generally greater than one, with higher estimates from AQ than SWF. The spatial variability in the distribution of the slopes was in good qualitative agreement with the CHL amplitude characteristic of each location. Slopes lower than one occurred generally in areas where CHL and its annual amplitude were <2 mg m^{-3}, whereas slopes greater than one were characteristic of productive waters where

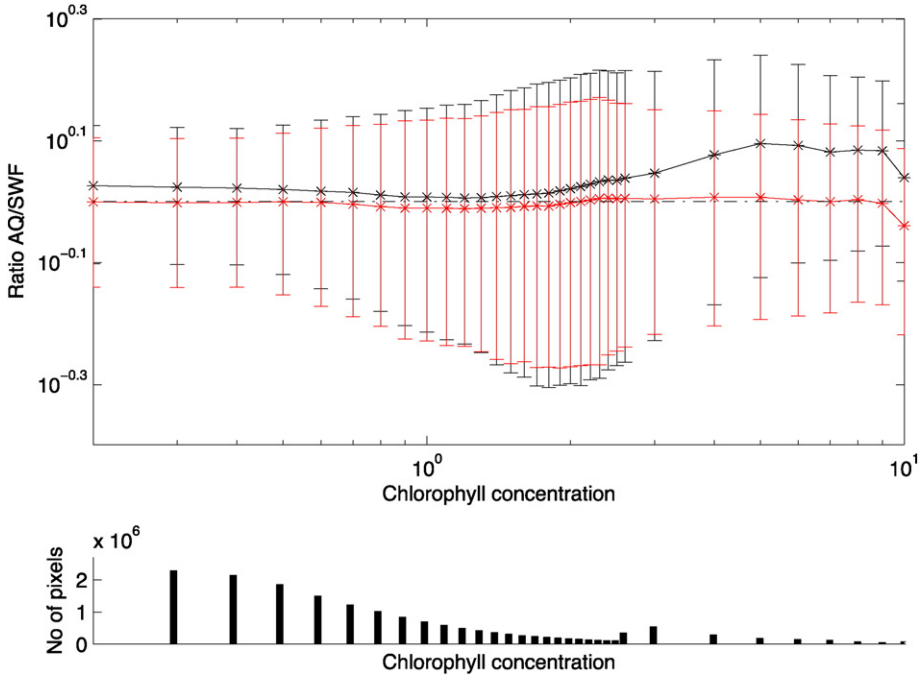

Fig. 4. Mean ratio AQ/SWF before (black) and after correction (red) as a function of chlorophyll concentration from SWF during 2002–2006 (54 months) for the entire study area (upper panel), and frequency distribution of the dataset (lower panel). Error bars in upper panel represent 1 standard deviation.

CHL reached high values and amplitudes were large (>2 mg m^{-3}) (Fig. 3b). These areas characterized by large amplitudes in CHL, such as mid-shelf waters and frontal systems, included 50% of the study area.

Although there was great spatial variability in the relationship between sensors, on average, retrievals from AQ were 10.4% larger than SWF for the study area, with a mean ratio AQ/SWF = 1.104 ± 0.377. In addition, the differences between SWF and AQ increased with CHL, with mean differences larger than 20% for CHL greater than 4 mg m^{-3} and a maximum of 25% for values between 5 and 6 mg m^{-3} (Fig. 4). Applying corrections at each pixel for the entire domain reduced the differences between sensors and resulted in an overall ratio AQ_{corr}/SWF = 1.040 ± 0.345. The distribution of errors showed the largest discrepancies between sensors in areas of high seasonal variability, such as the mid- and outer-shelf, which are generally associated with higher CHL during austral spring and summer, as well as in the oceanic area associated with the return of the Malvinas Current (Fig. 5). Waters in the inner continental shelf and the Malvinas Current had the lowest errors.

3.1. Spawning area (SUB)

The comparison of CHL from SWF and AQ at SUB between 2002 and 2006 also revealed important differences between sensors. Analyses of all individual pixels revealed that, on average, AQ values were 9.3% higher than SWF for the entire chlorophyll concentration range, with a mean ratio AQ/SWF = 1.093 ± 0.306 for SUB. After corrections were applied to the AQ dataset using the coefficients estimated from the relationships for 2002–2006, average CHL matched SWF estimates more closely, with an overall ratio AQ_{corr}/SWF = 1.025 ± 0.260 (Fig. 6). For CHL values between 1.5 and 3 mg m^{-3}, which include 24.67% of the data, the mean ratio AQ/SWF was reduced from 1.177 ± 0.424 to 1.030 ± 0.537, whereas for CHL >3 mg m^{-3}, which include 4.14% of the data at SUB and presumably represent the best conditions for zooplankton production and feeding of larval hake, ratios were reduced from 1.253 ± 0.536 to 1.072 ± 0.606 (Table 1).

The correction did not reduce the RMS at SUB considerably, but improved the agreement between sensors by eliminating biases and bringing the ratio AQ/SWF closer to one for all chlorophyll concentration ranges analyzed (Table 1, Fig. 6). The spatial distribution of errors showed that before correction, the largest errors were observed on the outer portion of the study area, in a band of high variability in CHL, where large values are often observed during spring and summer, but lower values occur during the rest of the year. In coastal areas characterized by low CHL throughout the year errors were generally smaller (Fig. 7).

3.2. Nursery area (SJG)

Results of the analysis of individual pixels at SJG indicated that for the entire chlorophyll concentration range (0.02–20 mg m^{-3}) AQ was 8.2% higher than SWF, with a mean ratio AQ/SWF = 1.082 ± 0.333. After correction, the overall ratio decreased to 1.034 ± 0.333 (Table 2). Analysis of different CHL ranges indicated that the overestimation of AQ relative to SWF held true for values between 0.02 and 3 mg m^{-3}, while for CHL >3 mg m^{-3} SWF produced slightly higher values than AQ (ratio AQ/SWF = 0.984 ± 0.411). Applying linear corrections improved the ratios between sensors and eliminated biases for all CHL ranges (Table 2, Fig. 8).

The spatial distribution of log_RMS showed an inverse pattern compared to SUB, with larger errors in coastal areas and better agreement between datasets toward the outer portions of the gulf (Fig. 9). Correction of the AQ dataset reduced log_RMS mostly in coastal waters shallower than 50 m.

3.3. Variability and trends in chlorophyll concentrations

The simple approach of estimating coefficients from linear regression between both sensors at each pixel and applying them to correct AQ data reduced RMS for most areas and chlorophyll concentration ranges, eliminated biases, and produced better agreement between sensors for the majority of the data. Thus, it is now suitable to combine both datasets to generate the longest time series of CHL available to date for the main reproductive area of *M. hubbsi*.

For the spawning area (SUB), the analysis of the extended time series of monthly mean CHL showed a marked seasonal cycle with maxima typically during October and November, a second peak during April, and minima in July and August (Fig. 10, top). Superimposed with this seasonal variability there was substantial interannual variability, with monthly mean values up to 4.89 mg m^{-3} in November 2014. A significant trend in chlorophyll concentrations was detected in this subregion, representing an increase of 2.33% per year, which is equivalent to an increase of 0.483 mg m^{-3} of the areal mean chlorophyll concentration from 1997 to 2015.

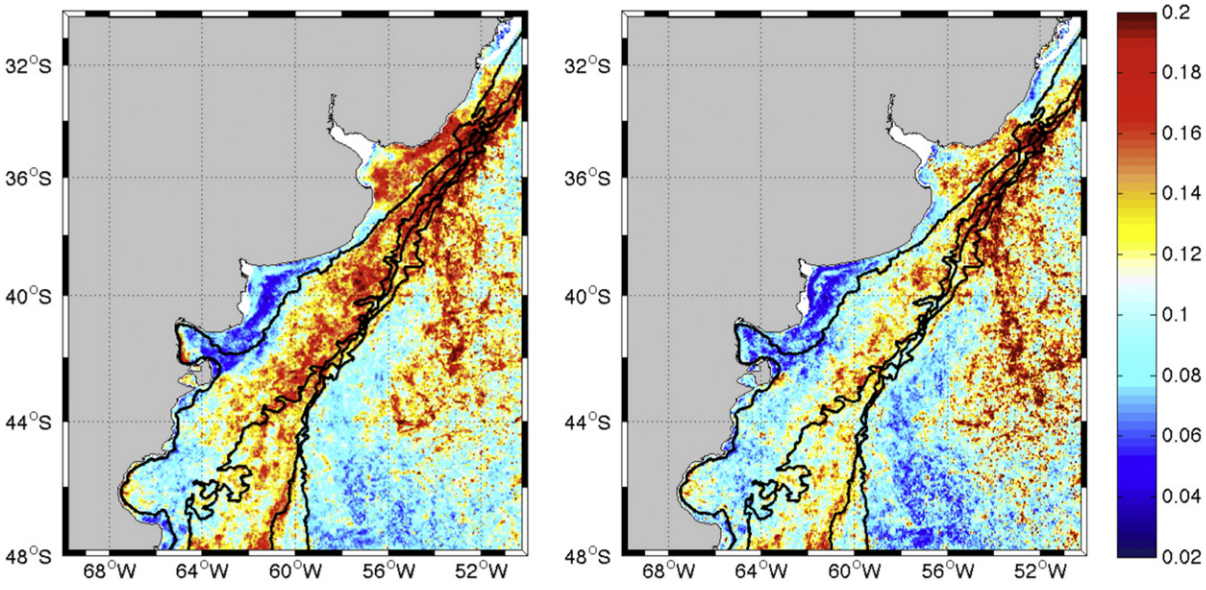

Fig. 5. Distribution of root mean square error (log_RMS) for the regression of SWF *vs.* AQ chlorophyll concentrations before (left) and after (right) correction at each pixel.

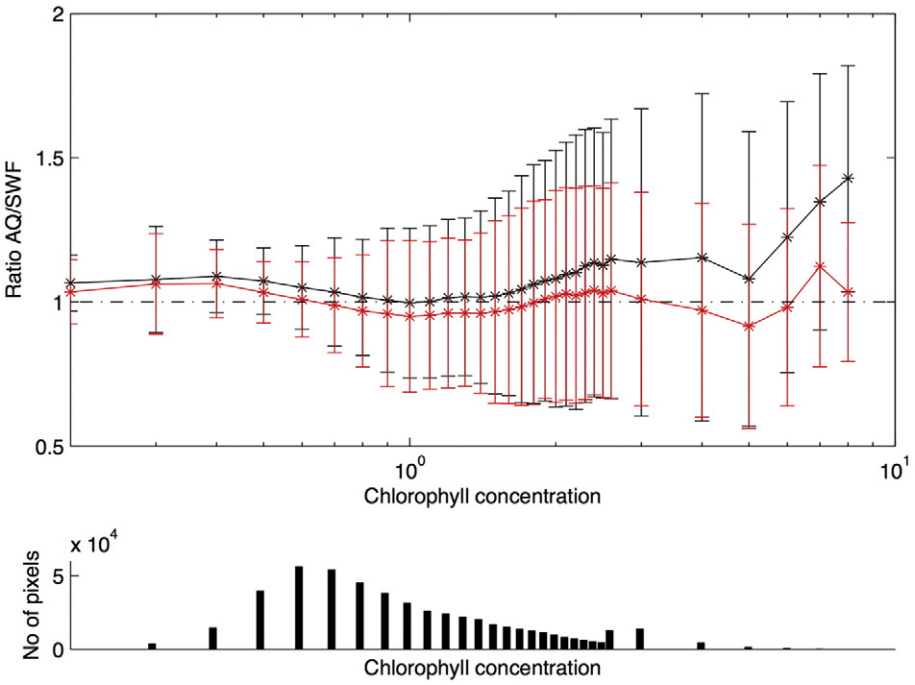

Fig. 6. Mean ratio of AQ/SWF before (black) and after correction (red) at SUB as a function of chlorophyll concentration (mg m^{-3}) from SWF between 2002 and 2006 (upper panel), and frequency distribution of the dataset (lower panel). Error bars in the upper panel represent 1 standard deviation.

At SJG, monthly mean CHL values were generally higher than those at SUB, with a less clear seasonal pattern and a maximum of 7.65 mg m^{-3} in October 2011 (Fig. 10, bottom). A positive trend was also detected in this subregion, indicating an average increase of 2.03% per year, which corresponds to an increase of 0.567 mg m^{-3} in the mean chlorophyll concentration of the area since 1997.

In addition to the generalized increasing trends in mean CHL observed at SUB and SJG, the analysis of individual pixels for the entire study area identified several areas of changing chlorophyll concentrations since 1997. There were significant trends at 19.25% of the pixels analyzed, with 97% of these being increases occurring mainly in coastal areas <50 m depth from 39 to 45°S, in the mid-shelf area off the San Jorge Gulf, and in deep oceanic waters east of the Malvinas Current between 40 and 48°S (Fig. 11). A small area with decreasing CHL was detected in oceanic waters with depths >1000 m between 34 and 40°S, but none was observed over the continental shelf. Most of the SUB area showed increasing CHL, with 81.29% of the pixels showing significant trends. At SJG 16.64% of the area showed increasing CHL, mostly in areas associated with the 50 m isobath.

4. Discussion

Driven by the need to ensure data continuity, merging and combining relatively short multi-sensor datasets has become an important goal of satellite oceanography (IOCCG, 2007). Our analyses showed that differences between SeaWiFS and MODIS retrievals in continental shelf and oceanic waters of the SWA were important and varied with the range of chlorophyll concentration, with maximum differences between sensors for the highest values. Previous studies have reported discrepancies between SeaWiFS and MODIS, with the largest differences also observed in highly productive waters including observations for the western South Atlantic. Dogliotti, Schloss, Almandoz, and Gagliardini (2009) compared SeaWiFS and MODIS retrievals for the SWA and reported relative percent errors between sensors ranging from 7 to 40%. Djavidnia, Melin, and Hoepffner (2010) examined standard products on global and regional scales based on monthly mean data between 2002 and 2009 and observed that in general, SeaWiFS produced higher chlorophyll concentration than MODIS in oligotrophic waters but there were a few areas where MODIS produced higher estimates than SeaWiFS, including the Patagonian shelf in summer. Overall, both sensors had similar variance and high correlation coefficients but results were spatially variable, indicating that global statistics are not applicable for regional studies. Franz, Bailey, Meister, and Werdell (2012) analyzed the quality and consistency of global chlorophyll concentration retrievals from SeaWiFS and MODIS and observed consistent estimates for the deep ocean relative to *in situ* measurements; however, sensors presented degraded agreement in higher productivity, higher complexity coastal regions where MODIS retrievals were biased high relative to SeaWiFS by 18%, on average.

Table 1
Statistics for the relationship SWF *vs.* AQ at SUB before and after correction for different chlorophyll concentration ranges (mg m^{-3}). Data were log-transformed before analyses. AQ/SWF ratios reported are means ± 1 standard deviation for the subregion.

	0.02–20	<0.5	0.5–1.5	1.5–3	>3
log_RMS	0.104	0.064	0.074	0.147	0.193
log_RMS_{corr}	0.093	0.056	0.071	0.129	0.155
log_bias	0.026	0.041	0.015	0.047	0.060
AQ/SWF ± SD	1.093 ± 0.306	1.106 ± 0.140	1.051 ± 0.220	1.177 ± 0.424	1.253 ± 0.536
AQ/SWF_{corr} ± SD	1.025 ± 0.260	1.009 ± 0.135	1.017 ± 0.236	1.030 ± 0.357	1.072 ± 0.606
n pixels	486,544	17,658	328,726	120,021	20,139
% pixels	100	3.63	67.56	24.67	4.14

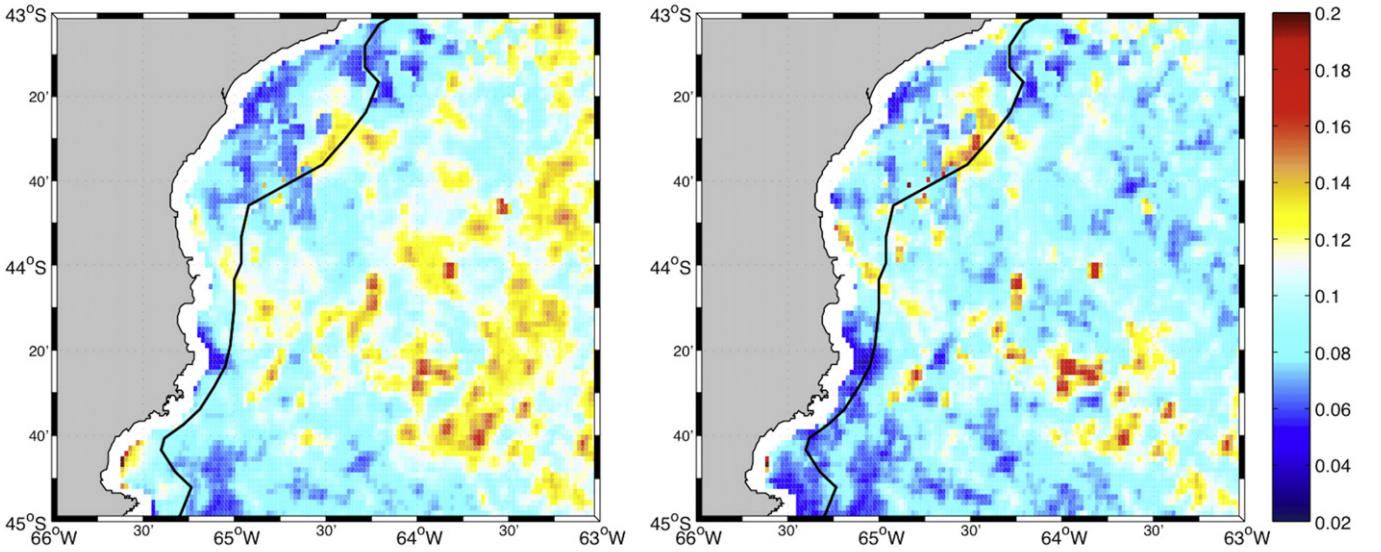

Fig. 7. Spatial distribution of the root mean square error (log_RMS) for the relationship between SWF and AQ chlorophyll concentrations before (left) and after (right) correction for SUB. The black line represents the 50 m isobath.

Several factors have been proposed as responsible for the differences observed in retrievals from multiple sensors (*e.g.*, McClain, 2009). For SeaWiFS and MODIS in particular, variations in chlorophyll concentrations may occur due to differences in the maximum band-ratio used in the standard algorithms. OC4v4 (SeaWiFS) makes use of a maximum band-ratio that incorporates 443, 490 and 510 nm. Likewise, OC3M (MODIS) makes use of a maximum-band-ratio, but only incorporates 443 and 488 nm wavelengths. As turbidity increases, the selected maximum-band migrates from shorter (blue) to longer (green) wavelengths. In the most turbid waters, OC4v4 selects 510 nm, while OC3M remains at 488 nm, which results in differences in the functional form of each algorithm that lead to large differences in chlorophyll retrievals at higher chlorophyll concentrations (Werdell et al., 2009; Franz et al., 2012). Earlier reports concluded that MODIS often produces better results than SeaWiFS due to reduced variability in the data, a higher signal-to-noise ratio, and improved spatial coverage (McClain, 2009). However, in highly productive areas such as the SWA where chlorophyll concentrations >5 mg m^{-3} are common and MODIS errors are larger than in oligotrophic waters, correcting MODIS data using SeaWiFS as a reference represents a better approach.

The spatial pattern observed in the relationship between SeaWiFS and MODIS largely coincided with the different oceanographic conditions in the area. South of 34°S, coastal waters shallower than 50 m are characterized by nitrate limitation and generally low phytoplankton abundances. The water column is vertically homogeneous throughout the year because tidal and wind-induced mixing overcomes surface heating (Martos & Piccolo, 1988; Carreto, Lutz, Carignan, Cuchi Colleoni, & De Marco, 1995). The mid-shelf presents seasonal vertical stratification, with a sharp thermocline overlying colder nutrient-rich waters during spring and summer. Both systems are separated by a tidal front established in proximity of the 50 m isobath in spring, where elevated concentrations of chlorophyll occur (Acha et al., 2004; Romero et al., 2006; Marrari et al., 2013). At the shelf-break, a sharp thermal front system develops in spring and summer, separating the relatively warm stratified shelf waters from colder nutrient-rich oceanic waters of the Malvinas Current (Romero et al., 2006), where other factors limit phytoplankton growth. At the location of the mid-shelf and shelf-break fronts, vertical velocities and retention are enhanced leading to increased production, strong spring–summer phytoplankton blooms, and large concentrations of zooplankton, fish, and higher trophic level organisms. The relationship between SeaWiFS and MODIS mostly matched these conditions, with better agreement between sensors in coastal waters <50 m deep and oceanic areas east of the Malvinas Current. These areas generally present lower chlorophyll concentrations and smaller seasonal amplitudes. On the other hand, slopes greater than unity, indicative of higher chlorophyll concentrations from MODIS relative to SeaWiFS, occurred primarily in the mid- and outer-shelf areas and in oceanic waters between 36 and 40°S, the latter generally associated with the southward return of the Malvinas Current. These areas are more productive and present higher seasonal amplitudes in chlorophyll concentrations. *In situ* values of up to >19 mg m^{-3} have been reported for continental shelf and shelf-break locations (*e.g.*, Almandoz et al., 2007; Schloss et al., 2007; Garcia et al., 2008; Bianchi et al., 2009).

Oceanic waters in the SWA are usually characterized by low phytoplankton abundances: while in the Malvinas Current light and weak vertical stratification presumably limit chlorophyll concentrations, the

Table 2
Statistics for the relationship SWF *vs.* AQ at SJG before and after correction of the AQ dataset for different chlorophyll concentration ranges (mg m^{-3}). Data were log-transformed before analyses. AQ/SWF ratios reported are means ± 1 standard deviation for the subregion.

	0.02–20	<0.5	0.5–1.5	1.5–3	>3
log_RMS	0.105	0.043	0.088	0.122	0.160
log_RMS_{corr}	0.106	0.056	0.091	0.125	0.143
log_bias	0.020	0.028	0.031	0.011	−0.037
AQ/SWF ± SD	1.082 ± 0.333	1.069 ± 0.081	1.096 ± 0.299	1.071 ± 0.378	0.984 ± 0.411
AQ/SWF_{corr} ± SD	1.034 ± 0.333	1.002 ± 0.068	1.024 ± 0.292	1.066 ± 0.552	0.991 ± 0.335
n pixels	324,175	5493	189,356	115,070	14,256
% pixels	100	1.69	58.41	35.50	4.4

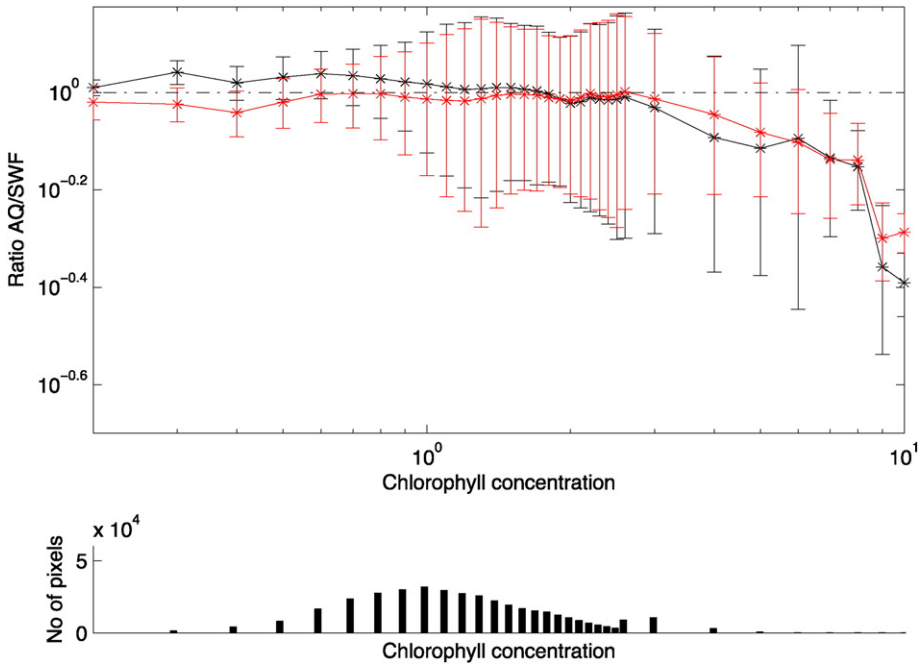

Fig. 8. Mean ratio of AQ/SWF before (black) and after correction (red) at SJG as a function of chlorophyll concentration (mg m^{-3}) from SWF between 2002 and 2006 (upper panel), and frequency distribution of the dataset (lower panel). Error bars in the upper panel represent 1 standard deviation.

warmer waters of the Brazil Current present low nutrient conditions. Therefore, the elevated amplitudes in chlorophyll concentrations observed in oceanic waters between 36 and 40°S must be supported by other processes. Brandini et al. (2000) postulated that mixing of warm, stratified, and low-nutrient subtropical waters with cold, well-mixed, and high-nutrient waters promotes the growth of phytoplankton along the Brazil/Malvinas Confluence. In addition, the oceanic area closer to the continental shelf, which includes the Brazil–Malvinas Confluence (BMC) and the return of the MC, has received special attention in recent years due to observations of significant water exchange between the shelf and the deep ocean (Piola, Moller, Guerrero, & Campos, 2008; Guerrero et al., 2014; Matano et al., 2014). Satellite derived surface salinity and numerical simulations revealed several events of off-shelf transport of low-salinity shelf water influenced by the Rio de la Plata, which can significantly enhance vertical stability. In addition, the BMC area is often characterized by meanders and eddies that can enhance productivity (Saraceno & Provost, 2012). High chlorophyll concentrations are often observed at the edges of meanders and warm-core eddies, where the warmer stable waters meet the nutrient rich MC. These events in oceanic waters are episodic, relatively short-lived, and variable in space and time. The intensity of these events and any associated trends are likely not represented accurately in the

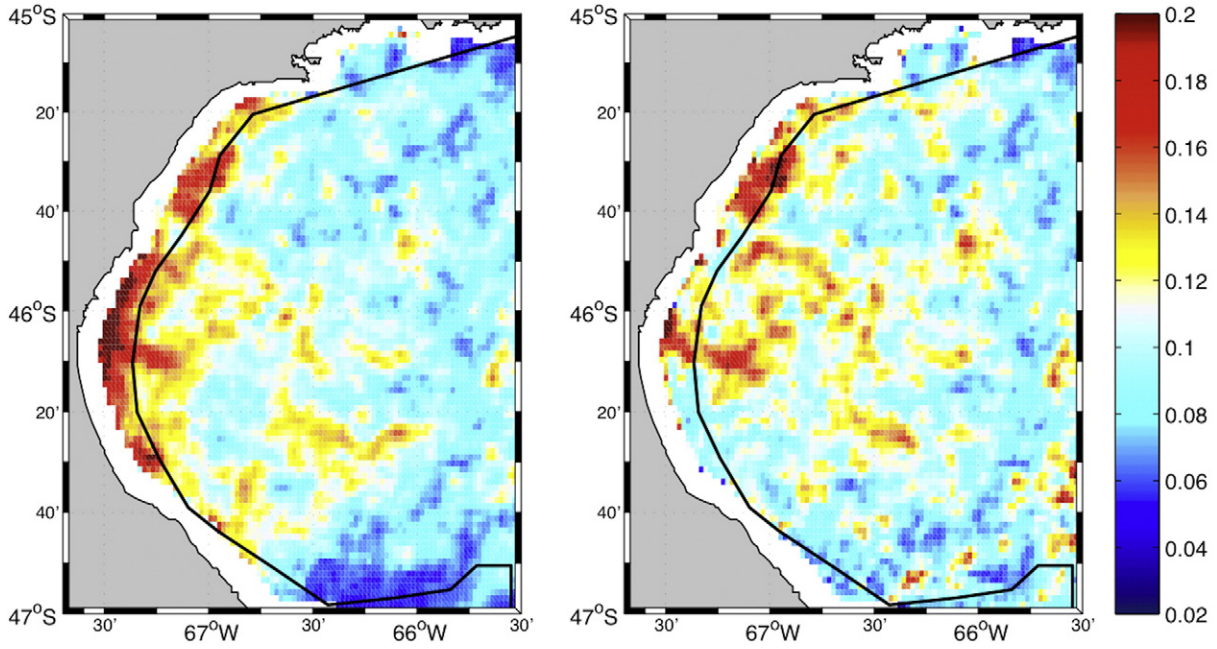

Fig. 9. Spatial distribution of the root mean square error (log_RMS) for the relationship between SWF and AQ chlorophyll concentrations before (left) and after (right) correction at SJG. The black line represents the 50 m isobath.

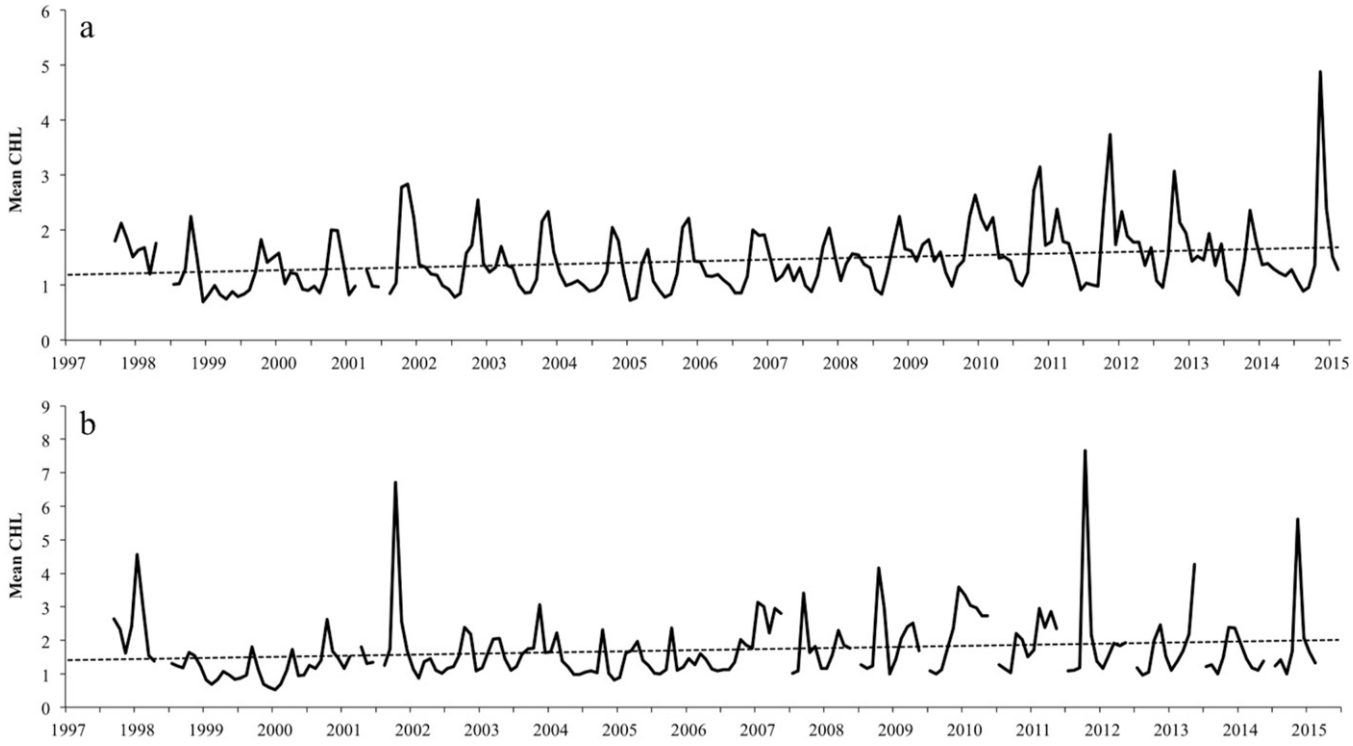

Fig. 10. Extended time series of monthly mean CHL (mg m^{-3}) at a) SUB and b) SJG for the period 1997–2015. Significant increasing trends were observed at SUB and SJG ($n = 210$). Trend significance was selected at 95% and assessed following the methodology described in Saulquin et al. (2013). The regression line is represented in black.

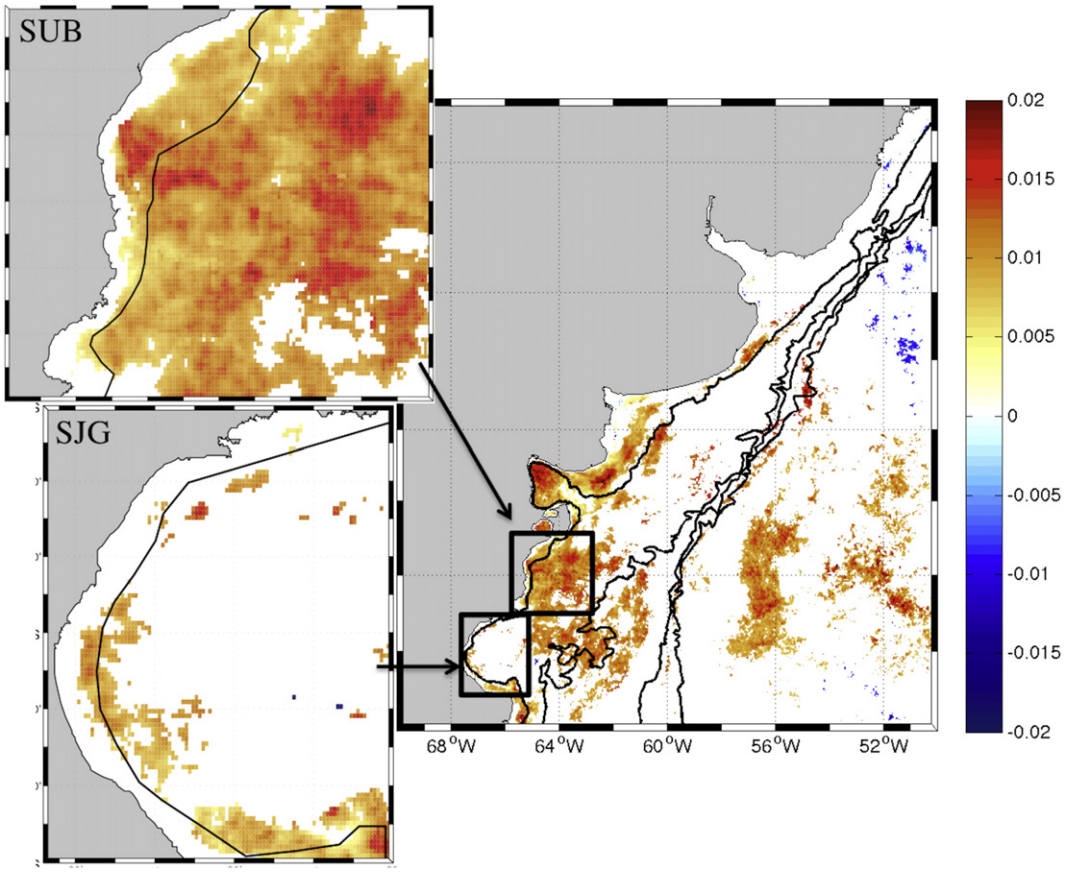

Fig. 11. Spatial distribution of significant trends in CHL (mg m^{-3} $year^{-1}$) in the study area for the period 1997–2015, with detailed views of SUB and SJG. Black lines represent the 50, 100, 200 and 1000 m isobaths. White areas indicate that the trend is not significantly different from zero at the 95% confidence level.

monthly composites used in our analyses. However, higher temporal resolution data revealed a significant number of these events since 1997 (*data not shown*), which had previously gone largely unnoticed. Future analyses of longer time series of CHL with finer resolution will allow the identification of the most predictable areas and timing of these events. These processes create localized favorable areas for phytoplankton growth, with potentially important implications for higher-trophic levels that may exploit increased food availability in normally food-poor areas (Godø et al., 2012). This might explain why elephant seals tend to forage along the Brazil/Malvinas Confluence and around eddies (Campagna, Piola, Marin, Lewis, & Fernández, 2006).

The newly extended chlorophyll time series, which is the longest to date for the SWA, revealed significant positive trends in several areas, including the main spawning ground of *M. hubbsi*, which were previously not identified in the data records derived from each sensor. Previous studies have observed either decreasing (Boyce, Lewis, & Worm, 2010) or increasing trends (Gregg, Casey, & McClain, 2005) in global mean chlorophyll concentrations, as well as regional and local changes. Gregg et al. (2005) reported a mean global increase in SeaWiFS chlorophyll concentrations of 4.1% for the period 1998–2003, with maximum contributions from coastal areas shallower than 200 m, including the Patagonian shelf. Gregg and Rousseau (2014) examined 15 years (1998–2012) of global chlorophyll concentration data resulting from the integration of satellite data, bias correction methods based on *in situ* data, and data assimilation, and found that although there were no significant trends in global mean chlorophyll, varying trends occurred in 6 of the 12 major oceanographic basins examined, including positive trends offshore of the Patagonian shelf and across the southern South Atlantic basin. Boyce et al. (2010) studied over a century of lower resolution global ocean transparency and *in situ* chlorophyll concentration data and observed decreasing chlorophyll concentrations in 60% of the world's ocean, although for the SWA region there was a positive trend. They also noted that most of these decreases occurred in oceanic areas, while in shelf regions trends switched from negative to positive trends since 1980, consistent with reported intensified coastal eutrophication and land runoff (Gregg et al., 2005). Saulquin et al. (2013) used SeaWiFS and MERIS data for the period 1998–2011 to assess the global distribution of trends and observed maximum increasing trends for the global ocean of 0.009 mg m^{-3} $year^{-1}$ on the Patagonian shelf.

Also recently, Siegel et al. (2013) analyzed over 13 years of global SeaWiFS data in 1° bins and observed some resemblance between the distributions of chlorophyll concentration trends and sea surface temperature (SST) trends. For the SWA area, trends in both SST and chlorophyll concentrations were mostly positive, although they typically occurred in oceanic waters. Our analyses focused on two coastal areas likely not properly resolved with the coarser resolution used in the Siegel et al. (2013) study. In addition, extending the time series by several years likely also contributed to detecting significant trends. The concurrent increases in SST and chlorophyll concentrations observed in the SWA are opposite to observations for other regions of the world's ocean where warmer surface temperatures were associated with decreasing chlorophyll concentrations (*e.g.*, Boyce et al., 2010). The effects of SST on chlorophyll may be explained through changes in mixed layer depth. Warmer SST leads to a shallower mixed layer and more intense stratification, which further limit nutrient supply to the surface (Behrenfeld et al., 2006). However, this may benefit phytoplankton at higher latitudes where growth is constrained by light availability and deep mixing. The Malvinas Current, a high-nutrient low-chlorophyll (HNLC) region, is characterized by strong turbulence and a vertically mixed structure, often interacting with the bottom topography. In this region nutrients are abundant but phytoplankton growth is limited by light. An increase in SST may enhance the vertical density gradient and contribute to maintaining phytoplankton cells in the illuminated layer during longer periods. Although there are no detailed analyses of sea surface temperature trends for this region, recent studies indicate global mean increases of 0.71 °C $century^{-1}$ since 1900 (Wu et al., 2012) and between 0.09° ± 0.03 and 0.18° ± 0.04 °C $decade^{-1}$ since the 1980s (Lawrence, Llewellyn-Jones, & Smith, 2004; Good, Corlett, Remedios, Noyes, & Llewellyn-Jones, 2007). A closer examination of the spatial variability in the trends reported in these studies reveals moderate increases for the SWA region, both in shelf and oceanic areas (Good et al., 2007; Belkin, 2009; Wu et al., 2012). The SWA warming along the southward extension of the Brazil Current is partly due to interdecadal changes in circulation, presumably associated with changes in basin-scale surface winds (*e.g.* Goni, Bringas, & DiNezio, 2011; Lumpkin & Garzoli, 2011). Such changes in circulation are also likely to alter nutrient availability and thus lead to CHL variability. On the other hand, for the reproductive area of *M. hubbsi* where seasonal stratification provides phytoplankton with an illuminated environment, the observed increase in chlorophyll concentrations is likely related to an enhanced nutrient supply, possibly as a result of eutrophication of coastal areas.

An overall increase in chlorophyll concentrations in the main reproductive area of *M. hubbsi* could have important implications. This species shows high interannual variability in egg production and larval survival, yet the factors that control these changes are not fully understood. High reproductive activity occurs during summer, when large concentrations of eggs and pelagic larvae are often observed at SUB. *M. hubbsi* is carnivorous throughout its life cycle, with adults feeding primarily on pelagic crustaceans, squid, and fish such as anchovy. Young larvae prey mainly on copepods while juveniles incorporate larger zooplankton (Viñas & Santos, 2000). A strong relationship has been observed between chlorophyll concentrations and zooplankton abundance in the spawning area of *M. hubbsi* (Temperoni, Viñas, Martos, & Marrari, 2014), as well as in other highly productive areas of the continental shelf, such as the main reproductive ground of the anchovy *Engraulis anchoita* (Marrari et al., 2013). High concentrations of calanoid copepodites and adults of *Drepanopus forcipatus*, *Ctenocalanus vanus*, and *Calanoides carinatus*, which are the preferred prey for hake larvae in the spawning area (Viñas & Santos, 2000; Temperoni & Viñas, 2013), also have been reported associated with high chlorophyll concentrations at the thermocline level (Derisio, 2012). It is reasonable to assume that chlorophyll concentrations are a good proxy for food availability for hake larvae and juveniles. Consequently, long-term increases in phytoplankton abundances in the reproductive area, where the highest abundances of larvae are observed, will likely have a positive impact on hake larval survival and recruitment. Interannual variability in phytoplankton dynamics has been previously shown to explain a large percentage of the changes observed in recruitment of other fish (Platt, Fuentes-Yaco, & Frank, 2003; Marrari et al., 2013) and crustaceans (Fuentes-Yaco, Koeller, Sathyendranath, & Platt, 2007; Marrari, Daly, & Hu, 2008). It is suggested that to better understand the variability of populations of *M. hubbsi*, future studies should include analyses of the changes over time in phytoplankton dynamics, including variations in the timing and duration of the spring–summer blooms, as well as of any associated changes in the composition and abundance of the dominant zooplankton of the area.

5. Conclusions

The results presented here provide unique information on the longer-term patterns of variability in chlorophyll concentrations in the Southwestern Atlantic Ocean and the reproductive grounds of hake *M. hubbsi* in particular. The analysis of the differences between SeaWiFS and MODIS chlorophyll retrievals in the SWA, the application of corrections and subsequent combination of datasets resulted in the longest high spatial resolution time series for the region, revealing significant trends in ~20% of the region that had gone previously undetected. The new dataset revealed large interannual variability and positive trends in chlorophyll concentrations for the spawning and nursery areas of *M. hubbsi* since 1997. These results highlight the usefulness of combining multi-sensor data for the assessment of ecosystem variability and

global change, and contribute to the goal of extending time series of key environmental parameters derived from satellite data.

Acknowledgements

We thank B. Franz, J. Werdell, and C. Hu for their input comments. The suggestions from two anonymous reviewers greatly improved this manuscript. SeaWiFS and MODIS data were distributed by the NASA Ocean Biology Processing Group. This study was partially funded by Fondo para la Investigación Científica y Tecnológica (Argentina) grants PICT-2013-1243 (MM), and PICT-2012-0467 (ARP). Additional funding was provided by project CRN3070 from the Inter-American Institute for Global Change Research through the US National Science Foundation grant GEO-1128040.

References

Acha, E.M., Mianzán, H.W., Guerrero, R.A., Favero, M., & Bava, J. (2004). Marine fronts at the continental shelves of austral South America. Physical and ecological processes. *Journal of Marine Systems*, *44*, 83–105.

Almandoz, G.O., Ferrario, M.E., Ferreyra, G.A., Schloss, I.R., Esteves, J.L., & Paparazzo, F.E. (2007). The genus *Pseudo-nitzschia* (Bacillariophyceae) in continental shelf waters of Argentina (Southwestern Atlantic Ocean, 38–55°S). *Harmful Algae*, *6*, 93–103.

Behrenfeld, M.J., O'Malley, R.T., Siegel, D.A., McClain, C.R., Sarmiento, J.L., Feldman, G.C., ... Boss, E.S. (2006). Climate-driven trends in contemporary ocean productivity. *Nature*, *444*, 752–755.

Belkin, I.M. (2009). Rapid warming of large marine ecosystems. *Progress in Oceanography*, *81*, 207–213.

Bezzi, S.I., Renzi, M., Irusta, G., Santos, B., Tringali, L.S., Ehrlich, M.D., ... Castrucci, R. (2004). Caracterización biológica y pesquera de la merluza (*Merluccius hubbsi*). In R.P. Sánchez, & S.I. Bezzi (Eds.), *El Mar Argentino y sus Recursos Pesqueros. Tomo 4. Los peces marinos de interés pesquero* (pp. 157–205). Mar del Plata, Argentina.: Publicaciones Especiales INIDEP (Instituto Nacional de Investigación y Desarrollo Pesquero).

Bianchi, A.A., Bianucci, L., Piola, A.R., Ruiz Pino, D., Schloss, I., Poisson, A., & Balestrini, C.F. (2005). Vertical stratification and air–sea CO_2 fluxes in the Patagonian shelf. *Journal of Geophysical Research*, *110*, C07003.

Bianchi, A.A., Ruiz Pino, D., Isbert Perlender, H.G., Osiroff, A.P., Segura, V., Lutz, V., ... Piola, A.R. (2009). Annual balance and seasonal variability of sea–air CO_2 fluxes in the Patagonian Sea: Their relationship with fronts and chlorophyll distribution. *Journal of Geophysical Research*, *114*, C03018.

Boyce, D.G., Lewis, M.L., & Worm, B. (2010). Global phytoplankton decline over the past century. *Nature*, *466*, 591–596.

Brandini, F., Boltovskoy, D., Piola, A.R., Kocmur, S., Rottgers, R., Abreu, P., & Mendes Lopes, R. (2000). Multiannual trends in fronts and distribution of nutrients and chlorophyll in the southwestern Atlantic. *Deep Sea Research, Part I*, *47*, 1015–1033.

Brunetti, N., Ivanovich, M., Aubone, A., and Rossi, G. 2000. Calamar (*Illex argentinu*). *In*: Síntesis del estado de las pesquerías marítimas argentinas y de la Cuenca del Plata. Mar del Plata, Argentina Bezzi, S.I., Akselman, R., and Boschi, E.E. (Eds), (1129 pp.).

Campagna, C., Piola, A.R., Marin, M.R., Lewis, M., & Fernández, T. (2006). Southern elephant seal trajectories, ocean fronts and eddies in the Brazil/Malvinas Confluence. *Deep Sea Research, Part I*, *53*, 1907–1924.

Campbell, J.W. (1995). The lognormal distribution as a model for bio-optical variability in the sea. *Journal of Geophysical Research*, *100*, 13237–13254.

Carreto, J.I., Lutz, V.A., Carignan, M.O., Cuchi Colleoni, A.D., & De Marco, S.G. (1995). Hydrography and chlorophyll *a* in a transect from the coast to the shelf-break in the Argentinian Sea. *Continental Shelf Research*, *15*, 315–336.

Cochrane, D., & Orcutt, G.H. (1949). Application of least squares regression to relationships containing auto-correlated error terms. *Journal of the American Statistical Association*, *44*(245), 32–61.

Cushing, D.H. (1974). The natural regulation of fish populations. In F.R. Harden Jones (Ed.), *Sea fisheries research* (pp. 399–412). United Kingdom: Elek Science. London.

Derisio, C. (2012). *El rol del frente de mareas de Península Valdés en el control de la comunidad zooplanctónica.* (PhD thesis) Argentina: Universidad Nacional de Mar del Plata (134 pp.).

Djavidnia, S., Melin, F., & Hoepffner, N. (2010). Comparison of global ocean colour data records. *Ocean Science*, *6*, 61–76.

Dogliotti, A.I., Schloss, I.R., Almandoz, G.O., & Gagliardini, D.A. (2009). Evaluation of SeaWiFS and MODIS chlorophyll-a products in the Argentinean Patagonian Continental Shelf (38°S–55°S). *International Journal of Remote Sensing*, *30*, 251–273.

Ehrlich, M.D., & de Ciechomski, J.D. (1994). Reseña sobre la distribución de huevos y larvas de merluza (*Merluccius hubbsi*) basada en veinte años de investigaciones. *Frente Marítimo*, *15*, 37–50.

Esaias, W.E., Abbott, M.R., Barton, I., Brown, O.B., Campbell, J.W., Carder, K.L., Clark, D.K., Evans, R.H., Hoge, F.E., Gordon, H.R., et al. (1998). An overview of MODIS capabilities for ocean science observations. *IEEE Transactions on Geoscience and Remote Sensing*, *36*, 1250–1265.

Franz, B.A., Bailey, S.W., Meister, G., & Werdell, P.J. (2012). Quality and consistency of the NASA Ocean color data record. *Proceedings of ocean optics XXI. Glasgow, Scotland, 8–12 October 2012*.

Fuentes-Yaco, C., Koeller, P.A., Sathyendranath, S., & Platt, T. (2007). Shrimp (*Pandalus borealis*) growth and timing of the spring phytoplankton bloom on the Newfoundland–Labrador Shelf. *Fisheries Oceanography*, *16*, 116–129.

Garcia, V.M.T., Garcia, C.A.E., Mata, M.M., Pollery, R., Piola, A.R., Signorini, S., ... Iglesias Rodriguez, M.D. (2008). Environmental factors controlling the phytoplankton blooms at the Patagonia shelf-break in spring. *Deep Sea Research, Part I*, *55*, 1150–1166.

Glorioso, P.D. (1987). Temperature distribution related to shelf-sea fronts on the Patagonian shelf. *Continental Shelf Research*, *7*, 27–34.

Godø, O.R., Samuelsen, A., Macaulay, G.J., Patel, R., Hjøllo, S.S., Horne, J., ... Johannessen, J.A. (2012). Mesoscale eddies are oases for higher trophic marine life. *PloS One*, *7*(1), e30161. http://dx.doi.org/10.1371/journal.pone.0030161.

Goni, G.J., Bringas, F., & DiNezio, P.N. (2011). Observed low frequency variability of the Brazil Current front. *Journal of Geophysical Research*, *116*, C10037. http://dx.doi.org/10.1029/2011JC007198.

Good, S.A., Corlett, G.K., Remedios, J.J., Noyes, E.J., & Llewellyn-Jones, D.T. (2007). The global trend in sea surface temperature from 20 years of advanced very high resolution radiometer data. *Journal of Climate*, *20*, 1255–1264.

Gregg, W.W., & Casey, N.W. (2004). Global and regional evaluation of the SeaWiFS chlorophyll dataset. *Remote Sensing of Environment*, *93*, 463–479.

Gregg, W.W., & Rousseau, C.S. (2014). Decadal trends in global pelagic ocean chlorophyll: a new assessment integrating multiple satellites, *in situ* data, and models. *Journal of Geophysical Research, Oceans*. http://dx.doi.org/10.1002/2014JC010158.

Gregg, W.W., Casey, N.W., & McClain, C.R. (2005). Recent trends in global ocean chlorophyll. *Geophysical Research Letters*, *32*, L03606. http://dx.doi.org/10.1029/2004GL021808.

Guerrero, R.A., Piola, A.R., Fenco, H., Matano, R.P., Combes, V., Chao, Y., ... Strub, P.T. (2014). The salinity signature of the cross-shelf exchanges in the Southwestern Atlantic Ocean: Satellite observations. *Journal of Geophysical Research, Oceans*, *119*, 7794–7810. http://dx.doi.org/10.1002/2014JC010113.

Hjort, J. (1914). Fluctuations in the great fisheries of northern Europe viewed in the light of biological research. *Rapp. P. V. Reun. Cons. Int. Explor. Mer*, *20*, 1–228.

Hu, C., Carder, K.L., & Müller-Karger, F.E. (2001). How precise are SeaWiFS ocean color estimates? Implications of digitization-noise errors. *Remote Sensing of Environment*, *76*, 239–249.

Hu, C.M., Muller-Karger, F.E., Taylor, C., Carder, K.L., Kelble, C., Johns, E., & Heil, C.A. (2005). Red tide detection and tracing using MODIS fluorescence data: A regional example in SW Florida coastal waters. *Remote Sensing of Environment*, *97*(3), 311–321.

IOCCG (2007). Ocean-colour data merging. In W.W. Gregg, J. Aiken, E. Kwiatkowska, S. Maritorena, F. Melin, H. Murakami, S. Pinnock, & C. Pottier (Eds.), *Report of the International Ocean Colour Coordinating Group. no. 6*, (68 pp., IOCCG, Dartmouth, Canada, 2007).

Lawrence, S.P., Llewellyn-Jones, D.T., & Smith, S.J. (2004). The measurement of climate change using data from the advanced very high resolution and along track scanning radiometers. *Journal of Geophysical Research*, *109*, C08017. http://dx.doi.org/10.1029/2003JC002104.

Legendre, P., & Legendre, L. (1998). *Numerical ecology* (2nd.edition). Amsterdam: Elsevier Scientific Publishing Company (870 pp.).

Lumpkin, R., & Garzoli, S. (2011). Interannual to decadal changes in the western South Atlantic's surface circulation. *Journal of Geophysical Research*, *116*, C01014. http://dx.doi.org/10.1029/2010JC006285.

Macchi, G.J., Martos, P., Reta, R., & Dato, C. (2010). Offshore spawning of the Argentine hake (*Merluccius hubbsi*) Patagonian stock. *Pan-American Journal of Aquatic Sciences*, *5*, 22–35.

Macchi, G.J., Pájaro, M., & Ehrlich, M. (2004). Seasonal egg production pattern of the Patagonian stock of Argentine hake (*Merluccius hubbsi*). *Fisheries Research*, *67*, 25–38.

Marrari, M., Daly, K.L., & Hu, C. (2008). Spatial and temporal variability of SeaWiFS chlorophyll *a* distributions west of the Antarctic Peninsula: Implications for krill production. *Deep Sea Research, Part II*, *53*, 377–392.

Marrari, M., Hu, C., & Daly, K.L. (2006). Validation of SeaWiFS chlorophyll *a* concentrations in the Southern Ocean: A revisit. *Remote Sensing of Environment*, *105*, 367–375.

Marrari, M., Signorini, S., McClain, C.R., Pájaro, M., Martos, P., Viñas, M.D., ... Buratti, C. (2013). Reproductive success of the Argentine anchovy, *Engraulis anchoita*, in relation to environmental variability at a mid-shelf front (Southwestern Atlantic Ocean). *Fisheries Oceanography*, *22*, 247–261.

Martos, P., & Piccolo, M.C. (1988). Hydrography of the Argentine continental shelf between 38° and 42°S. *Continental Shelf Research*, *8*, 1043–1056.

Matano, R.P., Combes, V., Piola, A.R., Guerrero, R., Palma, E.D., Strub, P.T., ... Saraceno, M. (2014). The salinity signature of the cross-shelf exchanges in the southwestern Atlantic Ocean: Numerical simulations. *Journal of Geophysical Research, Oceans*, *119*. http://dx.doi.org/10.1002/2014JC010116.

McClain, C.R. (2009). Satellite remote sensing: Ocean color. *Encyclopedia of ocean sciences* (pp. 4403–4416). United Kingdom: Elsevier Ltd. London.

McClain, C.R., Cleave, M.L., Feldman, G.C., Gregg, W.W., Hooker, S.B., & Kuring, N. (1998). Science quality SeaWiFS data for global biosphere research. *Sea Technology*, *39*, 10–16.

Muller-Karger, F.E., Varela, R., Thunell, R., Astor, Y., Zhang, H., & Hu, C. (2004). Processes of coastal upwelling and carbon flux in the CARIACO basin. *Deep Sea Research, Part II*, *51*, 927–943.

O'Reilly, J.E., Maritorena, S., O'Brien, M.C., Siegel, D.A., Toole, D., Menzies, D., Smith, R.C., Mueller, J.L., Mitchell, B.G., Kahru, M., et al. (2000). SeaWiFS postlaunch calibration and validation analyses: Part 3. SeaWiFS postlaunch technical report series. In S.B. Hooker, & Firestone R.E. (Eds.), *NASA technical memorandum 2000–206892. 11*, (49 pp.).

Pájaro, M., Macchi, G.J., & Martos, P. (2005). Reproductive pattern of the Patagonian stock of Argentine hake (*Merluccius hubbsi*). *Fisheries Research*, *72*, 97–108.

Palma, E.D., Matano, R.P., & Piola, A.R. (2008). A numerical study of the Southwestern Atlantic Shelf circulation: Stratified ocean response to local and offshore forcing. *Journal of Geophysical Research*, *113*, C11010. http://dx.doi.org/10.1029/2007JC004720.

Peterson, R.G., & Whitworth, T. (1989). The Subantarctic and Polar Fronts in relation to deep water masses through the southwestern Atlantic. *Journal of Geophysical Research*, *94*(C8), 10,817–10,838.

Piola, A.R., & Gordon, A.L. (1989). Intermediate waters in the southwest South Atlantic. *Deep-Sea Research*, *36*, 1–16.

Piola, A.R., Moller, O.O., Jr., Guerrero, R.A., & Campos, E.J.D. (2008). Variability of the subtropical shelf front off eastern South America: Winter 2003 and summer 2004. *Continental Shelf Research*, *28*, 1639–1648.

Platt, T., Fuentes-Yaco, C., & Frank, K.T. (2003). Spring algal bloom and larval fish survival. *Nature*, *423*, 398–399.

Rivas, A.L., & Pisoni, J.P. (2010). Identification, characteristics and seasonal evolution of surface thermal fronts in the Argentinean Continental Shelf. *Journal of Marine Systems*, *79*, 134–143.

Romero, S.I., Piola, A.R., Charo, M., & Garcia, C.A.E. (2006). Chlorophyll-*a* variability off Patagonia based on SeaWiFS data. *Journal of Geophysical Research*, *111*, C05021.

Sabatini, M.E., & Martos, P. (2002). Mesozooplankton features in a frontal area off northern Patagonia (Argentina) during spring 1995 and 1998. *Scientia Marina*, *66*(3), 215–232.

Sánchez, R.P., & Martos, P. (1989). Synopsis on the reproductive biology and early life history of *Engraulis anchoita*, and related environmental conditions in Argentine waters. *Second IOC Workshop on Sardine/Anchovy Recruitment Project (SARP) in the Southwest Atlantic, Montevideo, Uruguay. 65*. (pp. 7).

Saraceno, M., & Provost, C. (2012). On eddy polarity distribution in the southwestern Atlantic. *Deep Sea Research, Part I*, *69*, 62–69.

Saraceno, M., Provost, C., & Piola, A.R. (2005). On the relationship of satellite retrieved surface temperature fronts and chlorophyll-*a* in the Western South Atlantic. *Journal of Geophysical Research*, *110*, C11016. http://dx.doi.org/10.1029/2004JC002736.

Saraceno, M., Provost, C., Piola, A.R., Bava, J., & Gagliardini, A. (2004). Brazil Malvinas Frontal System as seen from 9 years of advanced very high resolution radiometer data. *Journal of Geophysical Research*, *109*, C05027.

Saulquin, B., Fablet, R., Mangin, A., Mercier, G., Antoine, D., & Fanton d'Andon, O. (2013). Detection of linear trends in multisensor time series in the presence of autocorrelated noise: Application to the chlorophyll-a SeaWiFS and MERIS data sets and extrapolation to the incoming Sentinel 3-OLCI mission. *Journal of Geophysical Research*, *118*, 3752–3763.

Schloss, I.R., Ferreira, G.A., Ferrario, M.E., Almandoz, G.O., Codina, R., Bianchi, A.A., ... Poisson, A. (2007). Role of plankton communities in sea–air variations in pCO_2 in the SW Atlantic Ocean. *Marine Ecology Progress Series*, *332*, 93–106.

Siegel, D.A., Behrenfeld, M.J., Maritorena, S., McClain, C.R., Antoine, D., Bailey, S.W., Bontempi, P.S., Boss, E.S., Dierssen, H.M., Doney, S.C., et al. (2013). Regional to global assessments of phytoplankton dynamics from the SeaWiFS mission. *Remote Sensing of Environment*, *135*, 77–91.

Simonazzi, M. (2003). Relación largo-peso y largo-edad de primera madurez sexual de la merluza. In L.S. Tringali, & S.I. Bezzi (Eds.), *Aportes para la evaluación del recurso merluza (Merluccius hubbsi) al sur de los 41°S. INIDEP technical report. 51*. (pp. 11–26).

Temperoni, B., & Viñas, M.D. (2013). Food and feeding of Argentine hake (*Merluccius hubbsi*) larvae in the Patagonian nursery ground. *Fisheries Research*, *148*, 47–55.

Temperoni, B., Viñas, M.D., & Buratti, C.C. (2013). Feeding strategy of juvenile (age-0 + year) Argentine hake *Merluccius hubbsi* in the Patagonian nursery ground. *Journal of Fish Biology*, *83*, 1354–1370.

Temperoni, B., Viñas, M.D., Martos, P., & Marrari, M. (2014). Spatial patterns of copepod biodiversity in relation to a tidal front system in the main spawning and nursery area of the Argentine hake *Merluccius hubbsi*. *Journal of Marine Systems*. http://dx.doi.org/10.1016/j.jmarsys.2014.08.015.

Tiao, G.C., Reinsel, G.C., Xu, D., Pedrick, J.H., Zhu, X., Miller, A.J., ... Wuebbles, D.J. (1990). Effects of autocorrelation and temporal sampling schemes on estimates of trend and spatial correlation. *Journal of Geophysical Research*, *95*(D12), 20507–20517.

Tonini, M., Palma, E., & Rivas, A. (2006). *Modelo de alta resolución de los golfos Patagónicos*. Mec. Comput., XXV, 1441–1460.

Viñas, M.D., & Santos, B.A. (2000). First-feeding of hake (*Merluccius hubbsi*) larvae and prey availability in the North Patagonian spawning area — Comparison with anchovy. *Archives of Fishery and Marine Research*, *48*, 242–254.

Weatherhead, E.C., Reinsel, G.C., Tiao, G.C., Meng, X., Choi, D., Cheang, W., Keller, T., DeLuisi, J., Wuebbles, D.J., Kerr, J.B., et al. (1998). Factors affecting the detection of trends: Statistical considerations and applications to environmental data. *Journal of Geophysical Research*, *103*(D14), 17,149–17,161.

Werdell, P.J., Bailey, S.W., Franz, B.A., Harding, L.W., Jr., Feldman, G.C., & McClain, C.R. (2009). Regional and seasonal variability of chlorophyll-*a* in Chesapeake Bay as observed by SeaWiFS and MODIS-Aqua. *Remote Sensing of Environment*, *113*, 1319–1330.

Wu, L., Cai, W., Zhang, L., Nakamura, H., Timmermann, A., Joyce, T., McPhaden, M.J., Alexander, M., Qiu, B., Visbeck, M., et al. (2012). Enhanced warming over the global subtropical western boundary currents. *Nature*. http://dx.doi.org/10.1038/NCLIMATE1353.